

See discussions, stats, and author profiles for this publication at: <https://www.researchgate.net/publication/6644474>

# Theory of high-order harmonic generation in relativistic laser interaction with overdense plasma

Article in *Physical Review E* · October 2006

DOI: 10.1103/PhysRevE.74.046404 · Source: PubMed

CITATIONS

331

READS

463

3 authors, including:



**Teodora Baeva**

Science and Technology Facilities Council

19 PUBLICATIONS 993 CITATIONS

[SEE PROFILE](#)



**A. Pukhov**

Heinrich-Heine-Universität Düsseldorf

432 PUBLICATIONS 19,654 CITATIONS

[SEE PROFILE](#)

Some of the authors of this publication are also working on these related projects:



Relativistic Coulomb clusters [View project](#)



Models for structured electron plasma acceleration [View project](#)

# Theory of high harmonic generation in relativistic laser interaction with overdense plasma

T. Baeva<sup>1</sup>, S. Gordienko<sup>1,2</sup>, A. Pukhov<sup>1</sup>

<sup>1</sup>*Institut für Theoretische Physik I, Heinrich-Heine-Universität Düsseldorf, D-40225, Germany*

<sup>2</sup>*L. D. Landau Institute for Theoretical Physics, Moscow, Russia*

(Dated: February 2, 2008)

High harmonic generation due to the interaction of a short ultra relativistic laser pulse with overdense plasma is studied analytically and numerically. On the basis of the ultra relativistic similarity theory we show that the high harmonic spectrum is universal, i.e. it does not depend on the interaction details. The spectrum includes the power law part  $I_n \propto n^{-8/3}$  for  $n < \sqrt{8\alpha}\gamma_{\max}^3$ , followed by exponential decay. Here  $\gamma_{\max}$  is the largest relativistic  $\gamma$ -factor of the plasma surface and  $\alpha$  is the second derivative of the surface velocity at this moment. The high harmonic cutoff at  $\propto \gamma_{\max}^3$  is parametrically larger than the  $4\gamma_{\max}^2$  predicted by the "oscillating mirror" model based on the Doppler effect. The cornerstone of our theory is the new physical phenomenon: spikes in the relativistic  $\gamma$ -factor of the plasma surface. These spikes define the high harmonic spectrum and lead to attosecond pulses in the reflected radiation.

PACS numbers: 42.65.Ky, 52.27.Ny, 52.38.Ph

## I. INTRODUCTION

High harmonic generation (HHG) from relativistically intense laser pulses interacting with solid targets has been identified as a promising way to generate bright ultra short bursts of X-rays [1, 2, 3]. For the first time this spectacular phenomenon was observed with nanosecond pulses of long wavelength (10.6  $\mu\text{m}$ ) CO<sub>2</sub> laser light [4].

Short after the experimental observation in 1981, Bezzlerides *et al* studied the problem of harmonic light emission theoretically [5]. Their approach based on non-relativistic equations of motion and hydrodynamic approximation for the plasma predicted a cutoff of the harmonic spectrum at the plasma frequency.

10 years later, in 1993, a new approach to the interaction of an ultra short, relativistically strong laser pulse with overdense plasma was proposed by Bulanov *et al* [6]. They "interpreted the harmonic generation as due to the Doppler effect produced by a reflecting charge sheet, formed in a narrow region at the plasma boundary, oscillating under the action of the laser pulse" [6]. The "oscillating mirror" model predicts a cutoff harmonic number of  $4\gamma_{\max}^2$ , where  $\gamma_{\max}$  is the maximal  $\gamma$ -factor of the mirror.

At the beginning of 1996 numerical results of particle-in-cell simulations of the harmonic generation by femtosecond laser-solid interaction were presented by P. Gibbon [7]. He demonstrated numerically that the high harmonic spectrum goes well beyond the cutoff predicted in [5] and also presented a numerical fit for the spectrum, which approximated the intensity of the  $n$ -th harmonic as  $I_n \propto n^{-5}$ . At about the same time the laser-overdense plasma interaction was also studied by Lichters *et al* [8].

The same year the analytical work by von der Linde and Rzazewski [9] appeared. The authors used the "oscillating mirror" model and approximated the oscillatory motion of the mirror as a sin-function of time without analysis of the applicability of this approximation. With

the explicit form of the mirror motion an analytical formula for the harmonic spectrum was obtained.

The first try to describe analytically the high harmonics generated at the boundary of overdense plasma by a short ultra intense laser pulse in a universal way that does not rely on an explicit formula for the exact plasma mirror motion was made in [1]. This work proposed for the first time the idea of universality of the harmonic spectrum. In an attempt to advocate the "oscillating mirror" model and the role of the relativistic Doppler effect the authors of [1] made use of the steepest descent method and estimated the harmonic spectrum as  $I_n \propto n^{-5/2}$ . However they did not discuss the area of applicability of the steepest descent method for the specific problem. We are showing in this article that applying the straightforward steepest descent method is equivalent to applying the "oscillating mirror" model that proves to be insufficient for the treatment of laser-overdense plasma interaction. In the present work we revise [1] and clarify the physical picture of HHG.

For the last couple of years the interest in the process of high harmonic generation from plasmas has enjoyed a revival thanks to the increasing interest in attoscience. The recent impressive progress in the physics of attosecond X-ray pulses [10] triggers the fascinating question whether a range of even shorter ones is achievable with the contemporary or just coming experimental technology.

L. Plaja *et al* [12] were the first to realize that the simple concept of the "oscillating mirror" gives an opportunity to produce extremely short pulses and presented a numerical proof that the radiation generated by oscillating plasma surfaces comes in the form of subfemtosecond pulses. For the first time the idea to use the plasma harmonics for the generation of subattosecond pulses (zeptosecond range) was announced in [1].

The present article improves the analytical results of [1] and studies in detail the ultra relativistic plasma surface

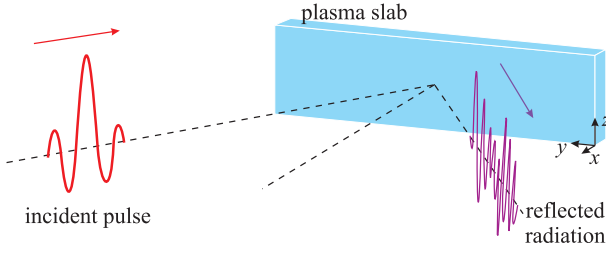


FIG. 1: Geometry of the problem. The laser pulse is moving towards the overdense plasma slab,  $x$  is perpendicular to the surface,  $y$  and  $z$  are parallel to it.

motion. We show that the high harmonics are generated due to sharp spikes in the relativistic  $\gamma$ -factor of the plasma surface. This new physical phenomenon leads to the spectrum cutoff at the harmonic number  $n_{\text{cutoff}}$

$$n_{\text{cutoff}} = \sqrt{8\alpha}\gamma_{\text{max}}^3. \quad (1)$$

The cutoff (1) is much higher than the  $4\gamma_{\text{max}}^2$ -cutoff predicted by the simple "oscillating mirror" model. Here  $\gamma_{\text{max}}$  is the maximum  $\gamma$ -factor of the surface and  $\alpha$  is a numerical factor of the order of unity, related to the plasma surface acceleration.

Our analysis significantly exploits the relativistic plasma similarity theory [15], which was developed after the work [1] had been published. The similarity theory enables us to rectify our previous results and to present them in a straightforward and clear way.

In this article we first discuss the physical picture of high harmonic generation. The production of high harmonics is attributed to the new physical effect of the relativistic spikes. Then, we develop analytical theory describing the spectrum of the high harmonics and show that this spectrum is universal with slow power law decay. Finally, the theory is confirmed by direct particle-in-cell (PIC) simulation results.

## II. PHYSICAL PICTURE OF HHG AT OVERDENSE PLASMA BOUNDARY

In this Section we state the problem of high harmonic generation at the boundary of overdense plasma and qualitatively describe its main features, which will find their analytical and numerical confirmation in what follows.

Let us consider a short laser pulse of ultra relativistic intensity, interacting with the sharp surface of an overdense plasma slab (see Fig. 1).

We assume that the incident laser pulse is short, so that we can neglect the slow ion dynamics and consider the electron motion only. The electrons are driven by the laser light pressure, a restoring electrostatic force comes from the ions. As a consequence, the plasma surface oscillates and the electrons gain a normal momentum component.

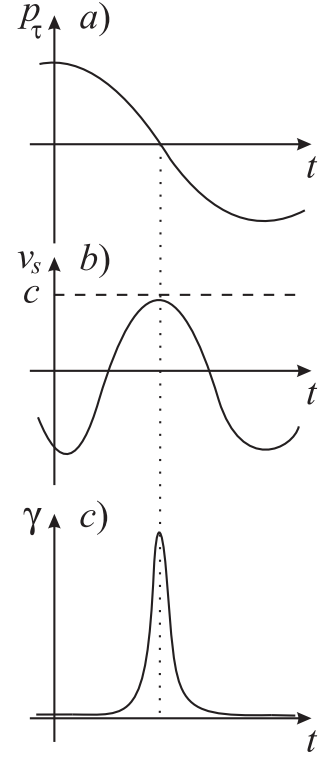


FIG. 2: a) Electron momentum component parallel to the surface as a function of time b) The velocity of the plasma surface  $v_s$  is a smooth function of time, unlike the  $\gamma$ -factor of the surface c)

Since the plasma is overdense, the incident electromagnetic wave is not able to penetrate it. This means that there is an electric current along the plasma surface. For this reason, the momenta of electrons in the skin layer have, apart from the components normal to the plasma surface, also tangential components.

According to the relativistic similarity theory [15], both the normal and tangential components are of the order of the dimensionless electromagnetic potential  $a_0$ . Consequently, the actual electron momenta make a finite angle with the plasma surface for most of the times.

Since we consider a laser pulse of ultra relativistic intensity, the motion of the electrons is ultra relativistic. In other words, their velocities are approximately  $c$ . Though the motion of the plasma surface is qualitatively different: its velocity  $v_s$  is not ultra relativistic for most of the times but smoothly approaches  $c$  only when the tangential electron momentum vanishes (see Fig. 2b).

The  $\gamma$ -factor of the surface  $\gamma_s$  also shows specific behavior. It has sharp peaks at those times for which the velocity of the surface approaches  $c$  (see Fig. 2c). Thus, while the velocity function  $v_s$  is characterized by its smoothness, the distinctive features of  $\gamma_s$  are its quasi-singularities.

When  $v_s$  reaches its maximum and  $\gamma_s$  has a sharp peak, high harmonics of the incident wave are generated and can be seen in the reflected radiation. Physically this

means that the high harmonics are due to the collective motion of bunches of fast electrons moving towards the laser pulse [13].

These harmonics have two very important properties. First, their spectrum is universal. The exact motion of the plasma surface can be very complicated, since it is affected by the shape of the laser pulse and can differ for different plasmas. Yet the qualitative behavior of  $v_s$  and  $\gamma_s$  is universal, and since it governs the HHG, the spectrum of the high harmonics does not depend on the particular surface motion.

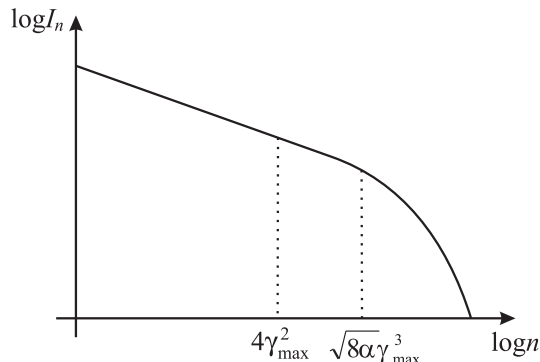


FIG. 3: The universal high harmonic spectrum contains power law decay and exponential decay (plotted in log-log scale).

We show below that the high harmonic spectrum contains two qualitatively different parts: power law decay and exponential decay (see Fig. 3). In the power law part the spectrum decays as

$$I_n \propto 1/n^{8/3}, \quad (2)$$

up to a critical harmonics number that scales as  $\gamma_{\max}^3$ , where  $I_n$  is the intensity of the  $n$ th harmonic (see Section V). Here  $\gamma_{\max}$  is the maximal  $\gamma$ -factor of the point, where the component of the electric field tangential to the surface vanishes (see Section IV).

The second important feature of the high harmonics is that they are phase locked. This observation is of particular value, since it allows for the generation of attosecond and even subattosecond pulses [1].

### III. ULTRA RELATIVISTIC SIMILARITY AND THE PLASMA SURFACE MOTION

The analytical theory presented in this work is based on the similarity theory developed in [15] for collisionless ultra relativistic laser-plasma regime and is valid both for under- and overdense plasmas.

The ultra relativistic similarity theory states that when the dimensionless laser vector potential  $\mathbf{a}_0 = e\mathbf{A}_0/mc^2$  is large ( $a_0^2 \gg 1$ ) the plasma electron dynamics does not

depend on  $a_0$  and the plasma electron density  $N_e$  separately. Instead they merge in the single dimensionless similarity parameter  $S$  defined by

$$S = \frac{N_e}{a_0 N_c}, \quad (3)$$

where  $N_c = \omega_0^2 m / 4\pi e^2$  is the critical electron density for the incident laser pulse with amplitude  $a_0$  and carrier frequency  $\omega_0$ .

In other words, when the plasma density  $N_e$  and the laser amplitude  $a_0$  change simultaneously, so that  $S = N_e/a_0 N_c = \text{const}$ , the laser-plasma dynamics remains similar. In particular, this basic ultra relativistic similarity means that for different interactions with the same  $S = \text{const}$ , the plasma electrons move along similar trajectories while their momenta  $\mathbf{p}$  scale as

$$\mathbf{p} \propto a_0. \quad (4)$$

The  $S$ -similarity corresponds to a multiplicative transformation group of the Vlasov-Maxwell equations, which appears in the ultra relativistic regime. The similarity is valid for arbitrary values of  $S$ . Physically the  $S$ -parameter separates relativistically overdense plasmas ( $S \gg 1$ ) from underdense ones ( $S \ll 1$ ).

To apply the key result (4) of the similarity theory to the plasma surface motion, we rewrite (4) for the electron momentum components that are perpendicular  $\mathbf{p}_n$  and tangential  $\mathbf{p}_\tau$  to the plasma surface:

$$\mathbf{p}_n \propto a_0, \quad \mathbf{p}_\tau \propto a_0. \quad (5)$$

This result is significant. It shows that when we increase the dimensionless vector potential  $a_0$  of the incident wave while keeping the plasma overdense, so that  $S = \text{const}$ , both  $\mathbf{p}_n$  and  $\mathbf{p}_\tau$  grow as  $a_0$ . In other words the velocities of the skin layer electrons

$$v = c \sqrt{\frac{\mathbf{p}_n^2 + \mathbf{p}_\tau^2}{m_e^2 c^2 + \mathbf{p}_n^2 + \mathbf{p}_\tau^2}} = c(1 - O(a_0^{-2})) \quad (6)$$

are about the speed of light almost at all times. Yet the relativistic  $\gamma$ -factor of the plasma surface  $\gamma_s(t')$  and its velocity  $\beta_s(t')$  behave in a quite different way. To realize this key fact let us consider the electrons at the very boundary of the plasma. The scalings (5) state that the momenta of these electrons can be represented as

$$\begin{aligned} \mathbf{p}_n(t') &= a_0 \mathbf{P}_n(S, \omega_0 t') \\ \mathbf{p}_\tau(t') &= a_0 \mathbf{P}_\tau(S, \omega_0 t'), \end{aligned} \quad (7)$$

where  $\mathbf{P}_n$  and  $\mathbf{P}_\tau$  are universal functions, which depend on the pulse shape and the  $S$ -parameter rather than on

$a_0$  or  $N_e$  separately. Consequently, for  $\beta_s(t')$  and  $\gamma_s(t')$  one obtains

$$\begin{aligned}\beta_s(t') &= \frac{p_n(t')}{\sqrt{m_e^2 c^2 + \mathbf{p}_n^2(t') + \mathbf{p}_\tau^2(t')}} \\ &= \frac{P_n(t')}{\sqrt{\mathbf{P}_n^2(t') + \mathbf{P}_\tau^2(t')}} - O(a_0^{-2}),\end{aligned}\quad (8)$$

$$\gamma_s(t') = \frac{1}{\sqrt{1 - \beta_s^2(t')}} = \sqrt{1 + \frac{\mathbf{P}_n^2(t')}{\mathbf{P}_\tau^2(t')}} + O(a_0^{-2}). \quad (9)$$

One sees from (6) that when  $a_0$  gets large, the relativistic  $\gamma$ -factor of the electrons becomes large too and their velocities approach the velocity of light. However, the dynamics of the plasma boundary is significantly different. For large  $a_0$ s the plasma boundary motion does not enter the ultra relativistic regime and its relativistic  $\gamma$ -factor  $\gamma_s(t')$  is generally of the order of unity. Yet there is one exception: if at the moment  $t'_g$  it happens that  $\mathbf{P}_\tau(S, t'_g) = 0$ , i.e.

$$\mathbf{p}_\tau(S, t'_g) = 0, \quad (10)$$

we have

$$\gamma_s = \frac{1}{\sqrt{1 - \beta_s^2}} = \sqrt{\frac{\mathbf{p}_n^2 + m_e^2 c^2}{m_e^2 c^2}} \propto a_0. \quad (11)$$

So the relativistic  $\gamma$ -factor of the boundary jumps to  $\gamma_s(t'_g) \propto a_0$  and the duration of the relativistic  $\gamma$ -factor spike can be estimated as

$$\Delta t' \propto 1/(a_0 \omega_0). \quad (12)$$

For the velocity of the plasma boundary one finds analogously that it smoothly approaches the velocity of light as  $\beta_s(t'_g) = (1 - O(a^{-2}))$ . Fig. 2 represents schematically this behavior.

As we will see later, the  $\gamma_s$  spikes cause the generation of high harmonics in the form of ultra short laser pulses.

#### IV. BOUNDARY CONDITION: ENERGY CONSERVATION AND THE APPARENT REFLECTION POINT

In this Section we introduce the boundary condition describing the laser-overdense plasma interaction appealing to physical arguments, just as it was previously done in [1, 12]. Mathematically rigorous analysis of the boundary condition is given in [13]. However, for the purposes of the present work it is sufficient to treat this problem on a more intuitive basis [1].

One might expect that the "oscillating mirror" model could describe the laser-plasma interaction in our problem. Therefore we want to explain in detail why it is not the case and then present the derivation of the correct boundary condition.

The "oscillating mirror" model implies that the tangential components of the vector potential are zero at the mirror surface. As a consequence, if the ideal mirror moves with  $\gamma \gg 1$  towards the laser pulse with the electric field  $E_l$  and the duration  $\tau_0$ , the reflected electric field will be  $E_{\text{refl}} \propto \gamma^2 E_l$  and the pulse duration will be  $\tau_{\text{refl}} \propto \tau_0/\gamma^2$ . The energy of the reflected pulse would be then  $\gamma^2$  times higher than that of the incident one. However, since the plasma surface is driven by the same laser pulse, this scaling is energetically prohibited and consequently the plasma cannot be described as an "ideal mirror".

To derive the correct boundary condition, let us consider the tangential vector potential components of a laser pulse normally incident onto a overdense plasma slab. These components satisfy the equation

$$\frac{1}{c^2} \frac{\partial^2 \mathbf{A}_\tau(t, x)}{\partial t^2} - \frac{\partial^2 \mathbf{A}_\tau(t, x)}{\partial x^2} = \frac{4\pi}{c} \mathbf{j}(t, x), \quad (13)$$

where  $\mathbf{A}_\tau(t, x = -\infty) = 0$  and  $\mathbf{j}$  is the tangential plasma current density. Eq. (13) yields

$$\mathbf{A}_\tau(t, x) = 2\pi \int_{-\infty}^{+\infty} \mathbf{J}(t, x, t', x') dt' dx'. \quad (14)$$

Here  $\mathbf{J}(t, x, t', x') = \mathbf{j}(t', x')(\Theta_- - \Theta_+)$ , where we have defined  $\Theta_- = \Theta(t - t' - |x - x'|/c)$  and  $\Theta_+ = \Theta(t - t' + (x - x')/c)$ , using the Heaviside step-function  $\Theta(t)$ . Due to this choice of  $\mathbf{J}$  the vector potential  $\mathbf{A}_\tau(t, x)$  satisfies both Eq. (13) and the boundary condition at  $x = -\infty$  since  $\mathbf{J}(t, x = -\infty, t', x') = 0$ . The tangential electric field is  $\mathbf{E}_\tau = -(1/c)\partial_t \mathbf{A}_\tau(t, x)$ . If we denote the position of the electron fluid surface by  $X(t)$  we have

$$\mathbf{E}_\tau(t, X(t)) = \frac{2\pi}{c} \sum_{\alpha=-1}^{\alpha=+1} \alpha \int_0^{-\infty} \mathbf{j}(t + \alpha\xi/c, X(t) + \xi) d\xi \quad (15)$$

where  $\xi = x' - X(t)$ .

Now one has to estimate the parameters characterizing the skin layer, i.e. the characteristic time  $\tau_s$  of skin layer evolution (in the co-moving reference frame) and the skin layer thickness  $\delta$ . Since the plasma is driven by the light pressure, one expects that  $\tau_s \propto 1/\omega_0$ . The estimation of  $\delta$  is more subtle. From the ultra relativistic similarity theory follows that  $\delta \propto (c/\omega_0) S^\Delta$ , where  $S \gg 1$  for strongly overdense plasmas and  $\Delta$  is an exponent that has to be found analytically. In this work we do not discuss the exact value of  $\Delta$ , but notice that this quantity does not depend on neither  $S$ , nor  $a_0$ . On the other hand, the

denser the plasma, the less the value of  $\delta$ . This condition demands that  $\Delta < 0$  and we get  $c/\omega_0 \gg \delta$  for  $S \gg 1$ .

If the characteristic time  $\tau_s$  of the skin layer evolution is long ( $c\tau_s \gg \delta$ ), then we can use the Taylor expansion  $\mathbf{j}(t \pm \xi/c, x' = X(t) + \xi) \approx \mathbf{j}(t, x') \pm \epsilon$ , where  $\epsilon = (\xi/c)\partial_t \mathbf{j}(t, x')$ , and substitute this expression into (15). The zero order terms cancel each other and we get  $\mathbf{E}_\tau(t, X(t)) \propto J_p(\delta/c\tau) \ll E_l$ , where  $J_p \propto cE_l$  is the maximum plasma surface current. Thus, as long as the skin-layer is thin and the plasma surface current is limited, we can use the Leontovich boundary condition [16]

$$\mathbf{e}_n \times \mathbf{E}(t, X(t)) = 0. \quad (16)$$

This condition has a straightforward relation to energy conservation. Indeed, if we consider the Poynting vector

$$\mathbf{S} = \frac{c}{4\pi} \mathbf{E} \times \mathbf{B}. \quad (17)$$

we notice that the boundary condition (16) represents balance between the incoming and reflected electromagnetic energy flux at the boundary  $X(t)$ .

The boundary condition (16) allows for another interpretation. An external observer sees that the electromagnetic radiation gets reflected at the point  $x_{\text{ARP}}(t)$ , where the normal component of the Poynting vector  $\mathbf{S}_n = c\mathbf{E}_\tau \times \mathbf{B}_\tau/4\pi = 0$ , implied by  $\mathbf{E}_\tau(x_{\text{ARP}}) = 0$ . We call the point  $x_{\text{ARP}}(t)$  the *apparent reflection point* (ARP).

The actual location of the ARP can be easily found from the electromagnetic field distribution in front of the plasma surface. The incident laser field in vacuum runs in the negative  $x$ -direction,  $\mathbf{E}^i(x, t) = \mathbf{E}^i(x + ct)$ , while the reflected field is translated backwards:  $\mathbf{E}^r(x, t) = \mathbf{E}^r(x - ct)$ . The tangential components of these fields interfere destructively at the ARP position  $x_{\text{ARP}}(t)$ , so that the implicit equation for the apparent reflection point  $x_{\text{ARP}}(t)$  is:

$$\mathbf{E}_\tau^i(x_{\text{ARP}} + ct) + \mathbf{E}_\tau^r(x_{\text{ARP}} - ct) = 0. \quad (18)$$

We want to emphasize that Eq. (18) contains the electromagnetic fields in vacuum. That is why the reflection point  $x_{\text{ARP}}$  is *apparent*. The real interaction within the plasma skin layer can be very complex. Yet, the external observer, who has information about the radiation in vacuum only, sees that  $\mathbf{E}_\tau = 0$  at  $x_{\text{ARP}}$ . The ARP is located within the skin layer at the electron fluid surface, which is much shorter than the laser wavelength for overdense plasmas, for which the similarity parameter is  $S \gg 1$ . In this sense, the ARP is attached to the oscillating plasma surface.

## V. HIGH HARMONIC UNIVERSAL SPECTRUM

According to Eq. (16), the electric field of the reflected wave at the plasma surface is

$$\mathbf{E}_r(t', X(t')) = -\mathbf{E}_i(t', X(t')), \quad (19)$$

where  $\mathbf{E}_i(t', X(t')) = -(1/c)\partial_{t'} \mathbf{A}_i(t', X(t'))$  is the incident laser field,  $t'$  is the reflection time. The one-dimensional wave equation translates signals in vacuum without change. Thus the reflected wave field at the observer position  $x$  and time  $t$  is  $\mathbf{E}_r(t, x) = -\mathbf{E}_i(t', X(t'))$ . Setting  $x = 0$  at the observer position we find that the Fourier spectrum of the electric field  $\mathbf{E}_r(t, x = 0)$  is

$$\mathbf{E}_r(\Omega) = \frac{m_e c \omega}{e \sqrt{2\pi}} \int_{-\infty}^{+\infty} \text{Re}[i\mathbf{a}((ct' + X(t'))/c\tau_0) \times \exp(-i\omega_0 t' - i\omega_0 X(t')/c)] \exp(-i\Omega t) dt, \quad (20)$$

where

$$t' - X(t')/c = t \quad (21)$$

is the retardation relation [8].

The fine structure of the spectrum of  $\mathbf{E}_r(t)$  depends on the particular surface motion  $X(t)$ , which is defined by the complex laser-plasma interaction at the plasma surface. Previous theoretical works on high order harmonic generation from plasma surfaces [7, 8, 9, 12] tried to approximate the function  $X(t)$  in order to evaluate the harmonic spectrum. For the first time analytical description of the high harmonic intensity spectrum and the concept of universality were presented in [1]. This work proclaims the idea that the most important features of the high harmonic spectrum do not depend on the detailed structure of  $X(t)$ . However, the article [1] treats the universal spectrum without any relation to similarity theory for ultra relativistic plasmas and, as a result, relies on the saddle-point method without proper analysis whether or not the areas contributing to the spectrum overlap [1, 17]. In our analysis we overcome these shortcomings of [1].

To find the spectrum, we notice that the investigation of  $\mathbf{E}_r(\Omega)$  (20) is equivalent to the investigation of the function

$$f(n) = f_+(n) + f_-(n), \quad (22)$$

where

$$f_\pm = \pm \int_{-\infty}^{+\infty} \mathbf{g}(\tau' + x(\tau')) \exp(\pm i(\tau' + x(\tau')) - in\tau) d\tau. \quad (23)$$

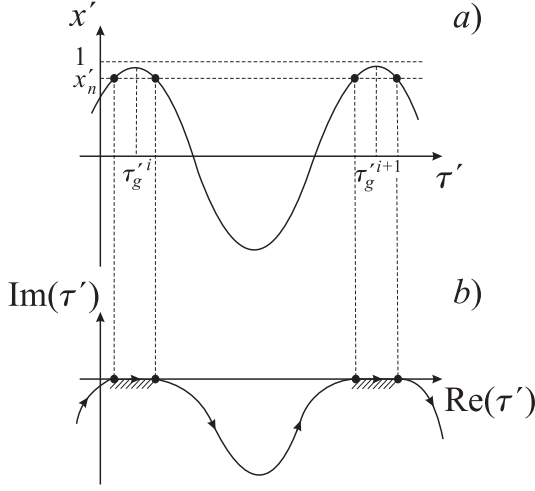


FIG. 4: Surface dynamics and path integration in (25). a) Velocity  $x'(\tau')$  of the plasma surface;  $x'_n = (n-1)/(n+1)$  are the saddle points corresponding to  $d\Theta/d\tau' = 0$ . b) The integration path can be shifted below the real axis everywhere except in the neighborhoods of  $\tau'_g$  (dashed regions).

Here  $\tau = \omega_0 t$ ,  $\tau' = \omega_0 t'$ ,  $n = \Omega/\omega_0$ ,  $x(\tau') = (\omega_0/c)X(t')$  and  $\mathbf{g}$  is a slowly varying function ( $|dg(\tau')/d\tau'| \ll 1$ ), which is trivially related to  $\mathbf{a}$  as

$$\mathbf{g}(\tau' + x(\tau')) = \frac{-im_e c}{2e\sqrt{2\pi}} \mathbf{a}((ct' + X(t'))/c\tau_0). \quad (24)$$

Making use of Eq. (21) we re-write Eq. (23) as

$$f_{\pm} = \pm \int_{-\infty}^{+\infty} g(\tau' + x(\tau')) \exp(i\tau'(-n \pm 1) + ix(\tau')(n \pm 1)) (1 - x'(\tau')) d\tau'. \quad (25)$$

We wish to examine the integral (25) for very large  $n$ . For this purpose, we notice that the derivative of the phase

$$\Theta(\tau') = \tau'(-n \pm 1) + x(\tau')(n \pm 1) \quad (26)$$

is negative everywhere except in the vicinity of  $\tau'_g = \omega_0 t'_g$  for which  $x'(\tau'_g) \approx 1$  (see Fig. 4a).

The physical meaning of  $\tau'_g$  and the behavior of  $x(\tau')$  in the vicinity of these times is explained by Eq. (10). Since the time derivative of  $\Theta(\tau')$  is negative for all  $\tau$ s that are not too close to one of the  $\tau'_g$ , we can shift the path over which we integrate to the lower half of the complex plane everywhere except in the neighborhoods of  $\tau'_g$  (see Fig. 4b). The contributions of the parts remote from the real axis are exponentially small. We can shift the path to the complex plane till the derivative equals zero or we find a singularity of the phase  $\Theta$ .

To calculate the contributions of  $\tau'_g$ 's neighborhoods we can expand  $x'(\tau')$  near each of its maxima at  $\tau'_g$ . Since

every smooth function resembles a parabola near its extrema, the expansion of  $x'(\tau')$  is a quadratic function of  $(\tau' - \tau'_g)$ . Simple integration leads to the following expression for  $x(\tau')$

$$x(\tau') = x(\tau'_g) + v_0(\tau'_g)(\tau' - \tau'_g) - \frac{\alpha(\tau'_g)}{3}(\tau' - \tau'_g)^3. \quad (27)$$

The Taylor expansion given by Eq. (27) has three important properties related to its dependence on  $S$  and  $a_0$ : 1) for  $S = \text{const}$  and  $a_0 \rightarrow +\infty$  one finds that  $v_0 \rightarrow c$ ; 2) for  $a_0 \rightarrow +\infty$ ,  $\alpha$  depends only on the parameter  $S$ ; 3) the expansion (27) is a good approximation for  $|\tau' - \tau'_g| \ll (2\pi/\omega_0)f_1(S)$ , where the function  $f_1$  does not depend on  $a_0$ . These three properties are mathematical statements of the physical picture described in Section II combined with the similarity theory developed in Section III. In other words, the properties of the expansion (27) just mentioned are direct consequences of the physical picture presented in Fig. 2.

Substitution of Eq. (27) into  $f_{\pm}(n)$  yields

$$f_{\pm}(n) = \sum_{\tau'_g} f_{\pm}(\tau'_g, n), \quad (28)$$

where the sum is over all times  $\tau'_g$ ,

$$f_+(\tau'_g, n) = g(\tau'_g + x(\tau'_g)) \exp(i\Theta_+(\tau'_g, n)) \times F(\tau'_g, n) \quad (29)$$

$$f_-(\tau'_g, n) = -g(\tau'_g + x(\tau'_g)) \exp(i\Theta_-(\tau'_g, n)) \times F(\tau'_g, -n) \quad (30)$$

$$F(\tau'_g, n) = \frac{4\sqrt{\pi}}{\alpha(\tau'_g)^{\frac{1}{3}} n^{\frac{4}{3}}} Ai\left(\frac{2}{n_{cr}(\tau'_g)} \frac{n - n_{cr}(\tau'_g)}{(\alpha(\tau'_g)n)^{1/3}}\right) \quad (31)$$

$$\Theta_{\pm} = \pm(\tau'_g + x(\tau'_g)) + n(x(\tau'_g) - \tau'_g), \quad (32)$$

and  $n_{cr} = 2/(1 - v_0)$ . In (31)  $Ai$  is the well-known Airy-function, defined as

$$Ai(x) = \frac{1}{\sqrt{\pi}} \int_0^{+\infty} \cos\left(ux + \frac{1}{3}u^3\right) du. \quad (33)$$

Note that if  $x(\tau' + \pi) = x(\tau')$  and  $g(\tau') = g(\tau' + \pi)$ , then  $f_{\pm}(2n) = 0$ .

Using equations (28)-(32) we can show analytically that the spectrum of radiation generated by the plasma is described by a universal formula.

For the intensity of the  $n$ th harmonic we obtain

$$I_n \propto |\exp(i\Theta_+(n)) F(n) - \exp(i\Theta_-(n)) F(-n)|^2, \quad (34)$$

where

$$F(n) = \frac{4\sqrt{\pi}}{(\sqrt[4]{\alpha n})^{4/3}} Ai\left(\frac{2}{n_{cr}} \frac{n - n_{cr}}{(\alpha n)^{1/3}}\right), \quad (35)$$

$$\Theta_{\pm}(n) = \pm\Theta_0 - n\Theta_1, \quad (36)$$

with the Airy function  $Ai(x)$  defined in (33) and the critical harmonic number  $n_{cr}$  satisfying  $n_{cr} = 4\gamma_{\max}^2$ , where  $\gamma_{\max}$  is the largest relativistic factor of the plasma boundary.

Eq. (34) gives an exact formula for the high harmonic spectrum, which includes both power law and exponential decay parts. Now we want to use different asymptotic representations of the Airy function in order to demonstrate explicitly these two quite different laws of high harmonic intensity decay.

For  $n < \sqrt{\alpha/8} n_{cr}^{3/2}$  ( $2|1 - n/n_{cr}| \ll (\alpha n)^{1/3}$ ) we can substitute the value of the Airy function at  $x = 0$  ( $Ai(0) = \sqrt{\pi}/(3^{2/3}\Gamma(2/3)) = 0.629$ ,  $Ai'(0) = -3^{1/6}\Gamma(2/3)/(2\sqrt{\pi}) = -0.459$ ) in Eq. (34), and obtain

$$I_n \propto \frac{1}{n^{8/3}} \left| \sin \Theta_0 + \frac{Ai'(0)}{Ai(0)} B(n, \Theta_0) \right|^2, \quad (37)$$

where

$$B(n, \Theta_0) = \frac{2 \sin \Theta_0}{(\alpha n_{cr})^{1/3}} \left( \frac{n}{n_{cr}} \right)^{2/3} + \frac{2i \cos \Theta_0}{(\alpha n)^{1/3}}. \quad (38)$$

This means that the universal spectrum

$$I_n \propto 1/n^{8/3} \quad (39)$$

is observed everywhere except for  $\sin \Theta_0 \approx 0$ , when the dominant term in the expansion is zero. For this particular case, a higher order correction is important for

$$(\alpha n)^{1/3} \tan \Theta_0 < 2 \left| \frac{Ai'(0)}{Ai(0)} \right| \quad (40)$$

and in this restricted frequency range the spectrum

$$I_n \propto 1/n^{10/3} \quad (41)$$

should be used.

At this point we want to explain the meaning of 8/3-spectrum universality. Notice that since Eq. (37) depends on the phase  $\Theta$ , for moderate values of  $n_{cr}$  the best power law fit of the high harmonic spectrum can be delivered by

$$I_n \propto n^{-p}, \quad (42)$$

where  $8/3 \leq p \leq 10/3$ . When  $n_{cr}$  becomes really large, the majority of the harmonics does not satisfy

the inequality (40) and the spectrum inevitably becomes  $I_n \propto n^{-8/3}$ . In other words, one should think of the 8/3-spectrum as the high intensity limit of the high harmonic spectrum. To find an analytical criterion for the 8/3-spectrum generation one can state that the condition (40) has to be violated for the harmonics with  $n \propto \sqrt{\alpha/8} n_{cr}^{3/2}$ . This means that

$$\gamma_{\max} > \gamma_{8/3} = \frac{1}{\sqrt{2} \tan \Theta_0} \left| \frac{Ai'(0)}{Ai(0)} \right|. \quad (43)$$

The formal expansion of the Airy function for  $n \ll n_{cr}$ ,  $(\alpha n)^{1/3} < 1$  leads to the spectrum  $I_n \propto 1/n^{5/2}$  discussed in [1]. Meticulous analysis demonstrates that this case is irrelevant. Yet the version of the saddle point method used in [1] ascribes the spectrum  $1/n^{5/2}$  to the whole area below the cutoff. This is because the areas around the saddle points contributing to the spectrum overlap significantly and the approximation used in [1] is not accurate enough in this part of the spectrum. However, the difference between the powers 8/3 and 5/2 is only 1/6 and it is hardly distinguishable numerically and experimentally.

For  $n > \sqrt{\alpha/8} n_{cr}^{3/2}$  ( $2|1 - n/n_{cr}| \gg (\alpha n)^{1/3}$ ) Eq. (31) can be rewritten as

$$I_n \propto \frac{n_{cr}^{1/2}}{n^3} \exp \left( -\frac{16\sqrt{2}}{3\alpha^{1/2}} \frac{n - n_{cr}}{n_{cr}^{3/2}} \right). \quad (44)$$

It is interesting to notice that the approximation used in [1] also gives Eq. (44) for this area, i.e. here the overlapping of the contributing areas is really negligible.

## VI. ULTRA SHORT PULSE DURATION

For ultra short pulse generation not only the amplitudes but also the harmonic phases are of importance. The calculations presented above show that all harmonics are phase locked. This means that after proper filtering they can produce a pulse of duration  $T$ , such that

$$T \propto \frac{\pi}{\omega_0} \frac{1}{\sqrt{\alpha n_{cr}^{3/2}}} \propto \frac{1}{\sqrt{\alpha} \gamma_{\max}^3}, \quad (45)$$

where  $\omega$  is the frequency of the fundamental wave.

Eq. (45) presents a new result. Notice that the plasma boundary never moves with a relativistic  $\gamma$ -factor larger than  $\gamma_{\max}$ . Consequently, the frequency of a photon reflected from this boundary due to the relativistic Doppler effect does not exceed  $4\gamma_{\max}^2 \omega_0 = n_{cr} \omega_0$ . How can a pulse with duration  $T$  given by Eq. (45) be produced then?

Mathematically this can be understood looking at the properties of the Airy function.  $Ai(x)$  changes its behavior from oscillatory for  $x < 0$  with  $|x| \gg 1$

$$Ai(x) \approx \frac{1}{|x|^{1/4}} \sin \left( \frac{2}{3} |x|^{3/2} + \frac{\pi}{4} \right) \quad (46)$$



to exponentially decaying for  $x \gg 1$

$$Ai(x) \approx \frac{1}{2x^{1/4}} \exp\left(-\frac{2}{3}x^{3/2}\right). \quad (47)$$

The point  $x = 0$  corresponds to  $n = n_{cr}$ . However, the exponential is so small for  $n < \sqrt{\alpha/8}n_{cr}^{3/2}$  that the power law decay dominates over the exponent. As a result, the power law spectrum goes well beyond the threshold  $\omega_0 n_{cr}$  predicted by oversimplified models considering reflection from a moving surface.

The reasoning just presented explains the mathematical origin of the  $\sqrt{\alpha/8}n_{cr}^{3/2}$ -cutoff. In the next section we give a simple physical interpretation of this result and reveal its relation to the relativistic  $\gamma$ -factor spikes. We also take a closer look at the mathematical nature of the cutoff and its relation to the failure of the standard saddle point approach due to saddle point overlapping.

## VII. RELATIVISTIC SPIKES AND CUT-OFF OF THE HIGH HARMONIC SPECTRUM

The  $\gamma^3$ -scaling of the spectrum cutoff (1) is readily understood using the relativistic  $\gamma$ -factor spikes of the plasma surface motion. Indeed, the plasma surface velocity in the vicinity of a maximum can be approximated as

$$v(t) = v_0(t_g) - \alpha\omega_0^2(t - t_g)^2 \quad (48)$$

(see Section V). Consequently, for the surface  $\gamma$ -factor during a relativistic spike we find

$$\gamma(t) \approx \frac{\gamma_{\max}}{\sqrt{1 + \gamma_{\max}^2 \alpha \omega_0^2 (t - t_g)^2}}, \quad (49)$$

where  $\gamma_{\max} = 1/\sqrt{1 - v_0^2(t_g)/c^2}$ . Eq. (49) shows that the highest harmonics are generated over the time interval

$$\Delta t \propto \frac{1}{\omega_0} \frac{1}{\sqrt{\alpha} \gamma_{\max}}. \quad (50)$$

For the whole time interval  $\Delta t$  the relativistic spike moves with ultra relativistic velocity in the direction of the emitted radiation. For this reason, the spatial length  $L$  of the high harmonic pulse produced is

$$L \propto (c - v_0(t_g))\Delta t \propto \frac{c}{\omega_0} \frac{1}{\sqrt{\alpha} \gamma_{\max}}. \quad (51)$$

A pulse of such duration contains frequencies

$$\Omega \propto \frac{c}{L} \propto \omega_0 \sqrt{\alpha} \gamma_{\max}^3, \quad (52)$$

what physically explains the origin of the high frequency cutoff (1). This cutoff should be compared with the one predicted by the "oscillating mirror" model:  $4\gamma_{\max}^2$ . It differs parametrically from the correct cutoff  $\propto \sqrt{8\alpha}\gamma_{\max}^3$ , which is due to the relativistic  $\gamma$ -factor spikes.

As it has been shown, the "oscillating mirror" model gives the incorrect formula for the spectrum cutoff because it does not include the relativistic  $\gamma$ -factor spikes. Mathematically, this failure "oscillating mirror" model is related to the saddle point overlapping. Eq. (26) defines the saddle points

$$\frac{dx(\tau')}{d\tau'} = 1 \pm \frac{1}{n}, \quad (53)$$

the vicinity of which determines the value of the integral describing the amplitude of the  $n$ -th harmonic,  $n \gg 1$ , see Fig. 4. Eq. (27) yields that the set of Eqs. (53) has real (not imaginary) solutions only for  $n < n_{cr} = 4\gamma_{\max}^2$ . For larger  $n$  all of the saddle points of (53) have an imaginary part.

Let us now apply the standard saddle point method to the problem without investigating whether the conditions for its applicability are met (it is clear that these conditions are violated at least for  $n \approx n_{cr}$ , for which two saddle points coincide). This approximation predicts that for  $1 \ll n \ll n_{cr}$  the spectrum decays as  $1/n^{5/2}$ . For  $n > n_{cr}$  this approach restores Eq. (47).

As it was mentioned above the spectrum  $1/n^{5/2}$  occurs formally in the limit  $(\alpha n)^{1/3} < 1$ . In other words, if  $\alpha$  were small, this spectrum would be observed. However, since  $\alpha$  depends on  $S$  rather than  $a_0$ , this spectrum corresponds to harmonics with small numbers only and is hardly of any practical interest. On the other hand, one can notice that  $\alpha$  describes the plasma surface acceleration at the maximum of the velocity. This means that the limit of small  $\alpha$  (and the spectrum  $1/n^{5/2}$ ) describes the limit of the surface moving without acceleration. However, this limit is of little interest for large  $a_0$ .

## VIII. CUTOFF AND THE STRUCTURE OF FILTERED PULSES

As we have seen, the relativistic plasma harmonics are phase locked and can be used to generate ultra short pulses. However, to extract these ultra short pulses, one has to remove the lower harmonics. The high energy cutoff (1) of the power law spectrum defines the shortest pulse duration that can be achieved this way.

Let us apply a high-frequency filter that suppresses all harmonics with frequencies below  $\Omega_f$  and study how the relative position of the  $\Omega_f$  and the spectrum cutoff affects the duration of the resulting (sub)attosecond pulses.

According to Eq. (34), the electric field of the pulse after the filtration is

$$E \propto \text{Re} \int_{\Omega_f/\omega_0}^{+\infty} (\exp(i\Theta_+(n)) F(n) - \exp(i\Theta_-(n)) \times \\ \times F(-n)) \exp(int) dn \quad (54)$$

The structure of the filtered pulses depends on where we set the filter threshold  $\Omega_f$ . In the case  $1 \ll \Omega_f/\omega_0 \ll \sqrt{\alpha/8} n_{cr}^{3/2}$ , we use Eq. (39) and rewrite Eq. (54) as

$$E \propto \text{Re} \int_{\Omega_f/\omega_0}^{+\infty} \frac{\exp(int)}{n^{4/3}} dn = \\ = \left( \frac{\omega_0}{\Omega_f} \right)^{1/3} \text{Re} \exp(i\Omega_f t - i\Theta_1) P(\Omega_f t), \quad (55)$$

where the function  $P$

$$P(x) = \int_1^{+\infty} \frac{\exp(iyx)}{y^{4/3}} dy \quad (56)$$

gives the slow envelope of the pulse.

It follows from the expression (55) that the electric field of the filtered pulse decreases very slowly with the filter threshold as  $\Omega_f^{-1/3}$ . The pulse duration decreases as  $1/\Omega_f$ . At the same time, the fundamental frequency of the pulse is  $\Omega_f$ . Therefore the pulse is hollow when  $\Omega_f/\omega_0 \ll \sqrt{\alpha/8} n_{cr}^{3/2}$ , i.e. its envelope is not filled with electric field oscillations. One possible application of these pulses is to study atom excitation by means of a single strong kick.

The pulses structure changes differ significantly when the filter threshold is placed above the spectrum cutoff. For  $\Omega_f/\omega_0 \gg \sqrt{\alpha/8} n_{cr}^{3/2}$  we use Eqs. (44) and (54) to obtain

$$E \propto \left( \frac{\omega_0}{\Omega_f} \right)^{3/2} \exp \left( -\frac{8\sqrt{2}\Omega_f}{3\sqrt{\alpha}\omega_0 n_{cr}^{3/2}} \right) \times \\ \times \text{Re} \frac{\exp(i\Omega_f t - i\Theta_1)}{8\sqrt{2}/(3\sqrt{\alpha} n_{cr}^{3/2}) + i\omega_0 t}. \quad (57)$$

The amplitude of these pulses decreases fast when  $\Omega_f$  grows. However, the pulse duration  $\propto 1/\sqrt{\alpha} n_{cr}^{3/2}$  does not depend on  $\Omega_f$ . Since the fundamental frequency of the pulse grows as  $\Omega_f$ , the pulses obtained with an above-cutoff filter are filled with electric field oscillations. Therefore these pulses are suitable to study the resonance excitation of ion and atom levels.

The minimal duration of the pulse obtained by cutting-off low order harmonics is defined by the spectrum cutoff  $\propto \sqrt{\alpha/8} n_{cr}^{3/2}$ . Physically, this result is the consequence of the ultra relativistic spikes in the plasma surface  $\gamma$ -factor.

## IX. SPECTRUM MODULATIONS

In this section we discuss the harmonic phases and show how the interference of harmonics produced by different  $\gamma$ -spikes can lead to spectrum modulations.

Eq. (28) obtained in Section V allows for straightforward physical interpretation. The sum  $f_-(\tau'_g, n) + f_+(\tau'_g, n)$  gives the contribution of the  $\tau'_g$ -spike of the surface relativistic factor to the harmonic spectrum (see Fig. 4). Therefore the phase of the  $n$ th harmonic  $\phi_n$  due to the  $\tau'_g$ 's spike is given by

$$\tan(\phi_n(\tau'_g) + n\Theta_1(\tau'_g)) \tan(\Theta_0) = \\ = \frac{1 - F(\tau'_g, -n)/F(\tau'_g, n)}{1 + F(\tau'_g, -n)/F(\tau'_g, n)}, \quad (58)$$

where  $\Theta_0(\tau'_g) = \tau'_g + x(\tau'_g)$  is the phase of the incident laser pulse at the time  $\tau'_g$  and  $\Theta_1(\tau'_g) = \tau'_g - x(\tau'_g) = \tau(\tau'_g)$ , the time of the observation, i.e. the symbol  $\Theta_1$  is redundant, yet we keep it for the sake of notation coherency.

Since  $F(\tau'_g, -n) \approx F(\tau'_g, n)$  for  $n \gg 1$ , Eq. (58) gives rise to  $\phi_n(\tau'_g) \approx -n\Theta_1(\tau'_g)$ . This means that each spike radiates phase locked high harmonics that can be used for ultra short pulse production. Another consequence of  $F(\tau'_g, -n) \approx F(\tau'_g, n)$  is that the amplitude of the harmonics is proportional to  $\sin(\Theta_0(\tau'_g))$ .

The mechanism presented in Fig. 2 has another very interesting consequence. Each harmonic is generated due to several spikes. These spikes contribute to (28) with different phase multipliers. This phase difference leads to modulations in the high harmonic spectrum. As an example we consider the interference between the harmonics produced by two different spikes in detail. The phase shift between the contributions from different spikes is  $\phi_n(\tau'_{g1}) - \phi_n(\tau'_{g2}) = \Theta_0(\tau'_{g1}) - \Theta_0(\tau'_{g2}) - n(\Theta_1(\tau'_{g1}) - \Theta_1(\tau'_{g2}))$  and can be large for large  $n$ . Since for  $n \ll \min(\sqrt{\alpha(\tau'_{g1})/8} n_{cr}^{3/2}(\tau'_{g1}), \sqrt{\alpha(\tau'_{g2})/8} n_{cr}^{3/2}(\tau'_{g2}))$  only  $Ai(0)$  enters  $f_{\pm}(\tau'_{g1,2})$ , the values of the contributions from the  $\tau'_{g1,2}$  spikes for this harmonic range do not depend on  $n_{cr}(\tau'_{g1,2})$ . As a result the modulations in this harmonic range depend only on the parameter  $S$ .

To recapitulate, the non-trivial plasma motion producing more than one  $\gamma$ -spike per oscillation period is the cause of the spectrum modulation.

## X. NUMERICAL RESULTS

In order to check our analytical results, we have performed a number of 1d PIC simulations with the 1d particle-in-cell code VLPL [18]. In all simulations a laser pulse with the Gaussian envelope  $a = a_0 \exp(-t^2/\tau_L^2) \cos(\omega_0 t)$ , duration  $\omega_0 \tau_L = 4\pi$  and dimensionless vector potential  $a_0 = 20$  was incident onto a plasma layer with a step density profile.

### A. Apparent Reflection Point

First, we study the oscillatory motion of the plasma and the dynamics of the apparent reflection point defined by the boundary condition (16) [20]. The plasma slab is initially positioned between  $x_R = -1.5\lambda$  and  $x_L = -3.9\lambda$ , where  $\lambda = 2\pi/\omega_0$  is the laser wavelength. The laser pulse has the amplitude  $a_0 = 20$ . The plasma density is  $N_e/N_c = 90$  ( $S = 4.5$ ).

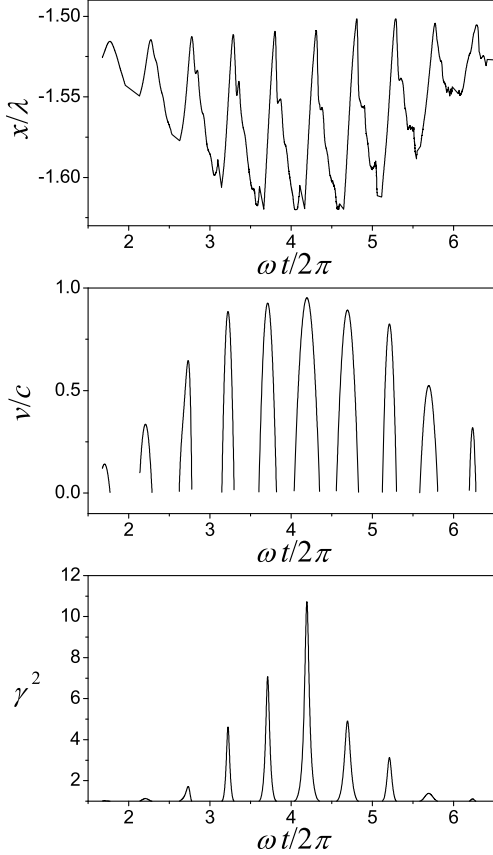


FIG. 5: 1D PIC simulation results for the parameters  $a_0 = 20$  and  $N_e = 90N_c$ . a) Oscillatory motion of the point  $x_{\text{ARP}}(t)$  where  $\mathbf{E}_r(x(t)) = 0$ . b) Velocity  $v_{\text{ARP}}(t) = dx_{\text{ARP}}(t)/dt$ ; only the positive velocities are shown, since they correspond to motion towards the laser pulse in the geometry of this simulation. Notice that the ARP velocity is a smooth function. c) The corresponding  $\gamma$ -factor  $\gamma_{\text{ARP}}(t) = 1/\sqrt{1 - v_{\text{ARP}}(t)^2/c^2}$  contains sharp spikes, which coincide with the velocity extrema.

At every time step, the incident and the reflected fields are recorded at  $x = 0$  (the position of the "external observer"). Being solutions of the wave equation in vacuum, these fields can be easily chased to arbitrary  $x$  and  $t$ . To find the ARP position  $x_{\text{ARP}}$ , we solve numerically equation (18). The trajectory of  $x_{\text{ARP}}(t)$  obtained in this simulation is presented in Fig. 5a. One can clearly see the

oscillatory motion of the point  $x_{\text{ARP}}(t)$ . The equilibrium position is displaced from the initial plasma boundary position  $x_R$  due to the mean laser light pressure.

Since only the ARP motion towards the laser pulse is of importance for the high harmonic generation, we cut out the negative ARP velocities  $v_{\text{ARP}}(t) = dx_{\text{ARP}}(t)/dt$  and calculate only the positive ones (Fig. 5b). The corresponding  $\gamma$ -factor  $\gamma_{\text{ARP}}(t) = 1/\sqrt{1 - v_{\text{ARP}}(t)^2/c^2}$  is presented in Fig. 5c. Notice that the ARP velocity is a smooth function. At the same time, the  $\gamma$ -factor  $\gamma_{\text{ARP}}(t)$  contains sharp spikes, which coincide with the velocity extrema. These numerical results confirm the predictions of the ultra relativistic similarity theory, which were presented in Section III.

### B. High harmonic spectrum

For the same laser-plasma parameters ( $a_0 = 20$ ,  $N_e = 90N_c$ ) the spectrum of high harmonic radiation is presented in Fig. 6. The maximum  $\gamma$ -factor of the apparent reflection point in this numerical simulation is  $\gamma_{\text{max}} \approx 3.3$  (compare with Fig. 5). Consequently the maximal harmonic number predicted by the "oscillating mirror" model lies at  $4\gamma_{\text{max}}^2 \approx 40$ , while the harmonic cutoff predicted by the relativistic spikes is about 100. Fig. 6 clearly demonstrates that there is no change of the spectrum behavior at  $4\gamma_{\text{max}}^2$ , while steeper decay takes place above 100, as predicted by our theory. Also, the spectral intensity modulations discussed in Section V and [3, 19] are observed.

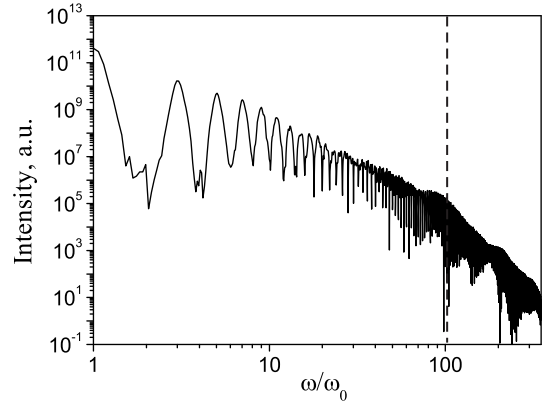


FIG. 6: Spectrum of high harmonics obtained numerically for the case of  $a_0 = 20$  and  $N_e = 90N_c$ , corresponding to  $S = 4.5$  and  $\gamma_{\text{max}} \approx 3.3$ . Assuming  $\alpha \approx 1$ , the cutoff (1) is expected at  $n \approx 100$ . This analytically predicted cutoff is marked by the dashed line.

To be able to make a real statement about the power in the power law decay of the spectrum we need more harmonics in order to satisfy the condition of universal 8/3-spectrum formation (43). For this reason we made

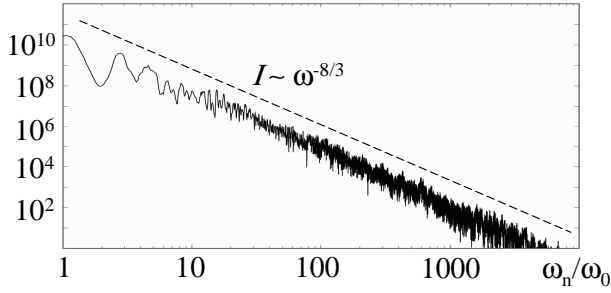


FIG. 7: Spectra of the reflected radiation for the laser amplitude  $a_0 = 20$  and the plasma density  $N_e = 30N_{cr}$ . The broken line marks the universal scaling  $I \propto \omega^{-8/3}$ .

the simulation with parameters  $a_0 = 20$  and  $N_e = 30N_{cr}$ , which roughly corresponds to solid hydrogen or liquid helium. The reflected radiation spectrum obtained for these parameters is shown in Fig. 7 in log-log scale. The power law spectrum  $I_n \propto 1/n^{8/3}$  is clearly seen here, thus confirming the analytical results of Section V.

### C. Subattosecond pulses

Let us take a closer look at Fig. 7. The power law spectrum extends at least till the harmonic number 2000, and zeptosecond ( $1\text{zs} = 10^{-21}\text{s}$ ) pulses can be generated. The temporal profile of the reflected radiation is shown in Fig. 8. When no spectral filter is applied, Fig. 8a, a train of attosecond pulses is observed [12].

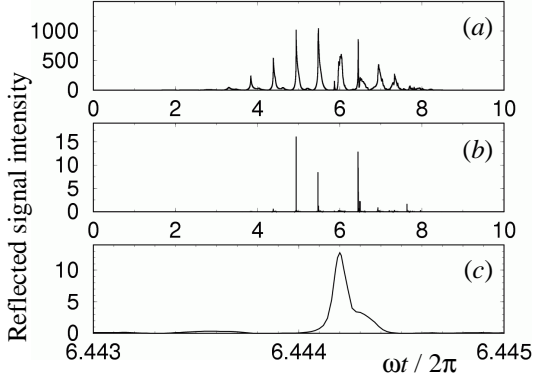


FIG. 8: Zeptosecond pulse train: a) temporal structure of the reflected radiation; b) zeptosecond pulse train seen after spectral filtering; c) one of the zeptosecond pulses zoomed, its FWHM duration is about 300 zs.

However, when we apply a spectral filter selecting harmonics above  $n = 300$ , a train of much shorter pulses is obtained, Fig. 8b. Fig. 8c zooms in to one of these pulses. Its full width at half maximum is about 300 zs. At the same time its intensity normalized to the laser frequency is huge  $(eE_{zs}/mc\omega)^2 \approx 14$ . This corresponds to the intensity  $I_{zs} \approx 2 \times 10^{19} \text{ W/cm}^2$ .

### D. Filter threshold and the attosecond pulse structure

The dependence of the short pulses on the position of the filter also can be studied numerically. We apply a filter with the filter function  $f(\omega) = 1 + \tanh((\omega - \Omega_f)/\Delta\omega)$ . It passes through frequencies above  $\Omega_f$  and suppresses lower frequencies. We choose the simulation case of laser vector potential  $a_0 = 20$  and plasma density  $N_e = 90N_{cr}$ . The spectrum of high harmonics is given in Fig. 6.

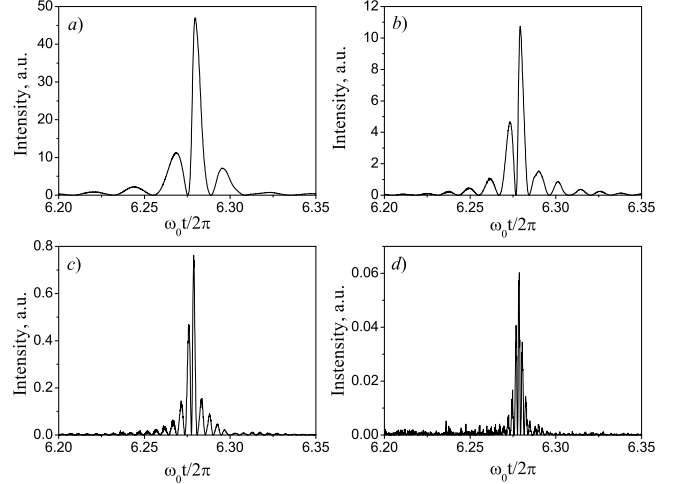


FIG. 9: Dependence of the pulses filling on the position of the sharp filter boundary for  $a_0 = 20$  and  $N_e = 90N_{cr}$  and filter positions: a)  $\Omega_f = 20\omega_0$ ,  $\Delta\omega = 2\omega_0$ ; b)  $\Omega_f = 40\omega_0$ ,  $\Delta\omega = 2\omega_0$ ; c)  $\Omega_f = 100\omega_0$ ,  $\Delta\omega = 2\omega_0$ ; d)  $\Omega_f = 200\omega_0$ ,  $\Delta\omega = 2\omega_0$

We zoom in to one of the pulses in the pulse train obtained and study how the shape of this one pulse changes with  $\Omega_f$ . Fig. 9 represents the pulse behavior for four different positions of  $\Omega_f$ . We measure the degree of fillness of the pulse by the number of field oscillations within the FWHM. One clearly sees that for filter threshold below the cutoff frequency, Fig. 9 a), b), the pulse is hollow. Notice that the case of Fig. 9b corresponds to the cutoff frequency predicted by the "oscillating mirror" model. Only for filter threshold positions above the spectrum cutoff given by (1) the pulse becomes filled, Fig. 9c,d. These results confirm once again the real position of the harmonic cutoff.

## XI. DISCUSSIONS

In this work we have shown analytically and numerically that the relativistic  $\gamma$ -factor spikes are the physical cause for high harmonic generation at the boundary of overdense plasma. It is important that the properties of

these spikes are universal and follow from the ultra relativistic similarity theory. The universal physics of the relativistic  $\gamma$ -spikes inheres in the universality of the high harmonic spectrum.

The spectrum of the high harmonics contains the power law part  $I_n \propto 1/n^{8/3}$ , which goes till the cutoff at  $\sqrt{8\alpha}\gamma_{max}^3$ . Here  $\gamma_{max}$  is the maximal  $\gamma$ -factor and  $\alpha$  describes the acceleration of the plasma boundary. This result demonstrates that a naive "oscillating mirror" model is insufficient for correct treatment of high harmonic generation at plasma boundaries.

It is interesting to note though that if the plasma

boundary moves without acceleration ( $\alpha \rightarrow 0$ ) our approach restores the cutoff  $4\gamma_{max}^2$  following from the "oscillating mirror" model and leads to  $I_n \propto 1/n^{5/2}$ , yet this limit is irrelevant to laser-relativistic plasma interaction.

## Acknowledgements

This work has been supported in parts by DFG Transregio 18 and by DFG Graduierten Kolleg 1203.

- 
- [1] S. Gordienko, A. Pukhov, O. Shorokhov and T. Baeva, Phys. Rev. Lett. **93**, 115002 (2004)
  - [2] G. D. Tsakiris, K. Eidmann, J. Meyer-ter-Vehn and F. Krausz, New J. Phys. **8**, 19 (2006).
  - [3] I. Watts *et al*, Phys. Rev. Lett. **88**, 155001-1 (2002)
  - [4] R. L. Carman, D. W. Forslund, J. M. Kindel, Phys. Rev. Lett., **46**, 29 (1981)
  - [5] B. Bezzerides, R. D. Jones, D. W. Forslund, Phys. Rev. Lett., **49**, 202 (1982)
  - [6] S. V. Bulanov *et al*, Phys. Plasmas, **1**, 745 (1993)
  - [7] P. Gibbon, Phys. Rev. Lett., **76**, 50 (1996)
  - [8] R. Lichters *et al*, Phys. Plasmas **3**, 3425 (1996)
  - [9] D. von der Linde, K. Rzazewski, Appl. Phys. B, **63**, 499 (1996)
  - [10] F. Krausz, Phys. World **14**, 41 (2001); M. Lewenstein, Science **297**, 1131 (2002); Ph. Bucksbaum, Nature (London) **421**, 593 (2003); N. A. Papadogiannis, B. Witzel, C. Kalpouzos, D. Charalambidis, Phys. Rev. Lett. **83**, 4289 (1999); A. Pukhov, S. Gordienko and T. Baeva, Phys. Rev. Lett. **91**, 173002 (2003).
  - [11] Y. I. Salamin, S. X. Su, Ch. H. Keitel, Phys. Reports **427**, 42 (2006).
  - [12] L. Plaja *et al*, J. Opt. Soc. Am. B **7**, 1904 (1998)
  - [13] T. Baeva, Diploma thesis: "Attosecond phenomena in laser-condensed matter interaction" (2005).
  - [14] J. D. Jackson, Classical Electrodynamics, Wiley, New York, 1999
  - [15] S. Gordienko and A. Pukhov, Phys. Plasmas **12**, 043109 (2005)
  - [16] L. D. Landau, E. M. Lifshitz, and L. P. Pitaevskii, Electrodynamics of Continuous Media, Pergamon Press, Oxford, 1984
  - [17] N. G. de Bruijn, Asymptotic methods in analysis, Dover, New York, 1981
  - [18] A. Pukhov, J. Plasma Phys., **61**, 425 (1999)
  - [19] U. Teubner *et al*, Phys. Rev. A, **67**, 013816 (2003)
  - [20] T. Baeva *et al*, submitted to PRL (January 2006) (arXiv:physics/0601044)